Environmental Science
Water Research & Technology

ROYAL SOCIETY OF CHEMISTRY

PAPER

View Article Online
View Journal | View Issue

Cite this: *Environ. Sci.: Water Res. Technol.*, 2021, **7**, 285

Emerging investigator series: emerging disinfection by-product quantification method for wastewater reuse: trace level assessment using tandem mass spectrometry†

Alejandro Ortega-Hernandez,[a] Raphael Acayaba,[b] Chad Verwold,[a] Cassiana Carolina Montagner[bc] and Susana Y. Kimura *[a]

The availability of freshwater sources is declining as a result of increasing populations, economic activities, and climate change. These increasing trends will also drive up the demand for potable water that will require the use of alternative sources including wastewater-impacted and saline waters. Therefore, it is crucial to understand the formation of emerging toxic DBPs from advanced treatment of treated secondary wastewater effluents for potable reuse. In this study, a highly sensitive analytical method was developed to characterize 25 DBPs from 5 chemical classes (haloacetonitriles, halonitromethanes, haloacetaldehydes, haloketones, and iodinated trihalomethanes) in recycled wastewaters using a gas chromatography tandem mass spectrometer (MS/MS). The high sensitivity of MS/MS technology permitted a reduced sample concentration factor (50×) that required only 30 min of extraction time and 10 mL of sample volume. Method detection limits are the lowest reported between 2.0–68.9 ng L^{-1}. Matrix effects in secondary wastewater effluents were low (0–30%) compared to ultra pure water. A full-scale facility for wastewater reuse that treated secondary wastewater effluents through microfiltration (UF), followed by ozone (UF/O_3) or reverse osmosis (UF/RO) was evaluated. Water samples from each process were chlorinated (HOCl) and chloraminated (NH_2Cl) to evaluate DBP precursor removal and DBP formation potential, the first study of its kind. Overall, HOCl formed higher summed DBP levels (0.5–18.5 μg L^{-1}) compared to NH_2Cl (0.2–8.5 μg L^{-1}). HAN was significantly lower in UF/O_3/HOCl (59%) and UF/RO/HOCl (99%) compared to UF/HOCl. However, HNM was enhanced after UF/O_3/HOCl. In chloraminated samples, UF/O_3/NH_2Cl produced a higher amount of DBPs compared to UF/NH_2Cl including haloacetonitriles, halonitromethanes, haloketones, and iodinated trihalomethanes.

Received 22nd October 2020,
Accepted 13th January 2021

DOI: 10.1039/d0ew00947d

rsc.li/es-water

Water impact

A highly sensitive analytical method was developed that simultaneously characterizes 25 unregulated DBPs from five chemical classes in wastewater effluents and recycled waters with the lowest reported detection limits. DBP formation potential with chlorine and chloramines was evaluated across a full-scale potable wastewater reuse facility for the first time.

1. Introduction

Water disinfection is used in drinking water and wastewater treatment to effectively control microbial pathogens that lead to waterborne diseases. However, organic matter and inorganic compounds (*i.e.* Br^-, I^-) that naturally occur in rivers and lakes can also react with disinfectants to produce disinfection by-products (DBPs). DBPs are always present in disinfected waters typically at μg L^{-1} levels.[1–5] Although disinfectants protect against immediate acute risks produced by microbial pathogens, DBPs may lead to potential chronic health problems caused by long-term exposure, including bladder cancer and adverse birth outcomes.[6–15] Currently, guidelines and regulations have been established globally for 12 DBPs including trihalomethanes (THMs) and haloacetic acids.[2–5,16] However, more than 700 DBPs have been identified in surface or groundwaters disinfected with chlorine, chloramines, ozone, and chlorine dioxide.[5,17,18]

[a] *Department of Chemistry, University of Calgary, 2500 University Dr. NW, Calgary, AB, Canada T2N 1N4. E-mail: s.kimurahara@ucalgary.ca*
[b] *School of Technology, University of Campinas, 13484-332 Limeira, SP, Brazil*
[c] *Institute of Chemistry, University of Campinas, 13083-970 Campinas, SP, Brazil*
† Electronic supplementary information (ESI) available. See DOI: 10.1039/d0ew00947d

Other DBP chemical classes include haloacetonitriles, halonitromethanes, haloacetaldehydes, haloketones, haloacetamides, and haloacids.

The chemical and biological composition of source waters used for drinking water purposes are constantly changing as the result of population growth, climate change, and water scarcity.[19] Anthropogenic compounds (*i.e.*, pharmaceuticals, personal care products, industrial chemicals) that are not well removed from treated wastewater are increasingly being found in lakes and rivers.[20,21] Disinfectants also react with anthropogenic compounds which can potentially produce a different suite of DBPs compared to pristine waters.[22,23] However, only a few studies have characterized the formation of unregulated priority DBPs (*i.e.*, haloacetonitriles, haloketones, haloaldehydes, halonitromethanes) in wastewater-impacted source waters and wastewater reuse.[24–32] Although recent toxicological studies suggest that disinfected wastewater-impacted waters are more toxic than pristine waters, advanced water treatment including reverse osmosis and advanced oxidation processes may reduce the overall toxicity.[33,34] It is critical to understand the efficiency of advanced and conventional treatment processes to remove or transform anthropogenic contaminants in source waters and bridging that knowledge gap to water toxicity. This is the first study that evaluates DBP precursor removal in a wastewater reuse facility.

Quantification of all DBP chemical classes could be laborious and intensive because most analytical methods are optimized for specific chemical and physical properties of a single DBP chemical class.[2–5] Multianalyte methods that combine distinct chemical classes of unregulated DBPs have been developed in recent years which facilitates comprehensive DBP analysis.[35–40] However, these methods are mostly used for drinking water matrices and have not been validated for wastewater-impacted waters. Wastewater effluents are complex matrices that may introduce matrix effects to methods used for drinking water matrices. Furthermore, as more studies evaluate the formation of unregulated DBPs from disinfection of pharmaceuticals, personal care products, and other environmental pollutants present in wastewater at parts per trillion levels, DBP analytical methods with higher sensitivity are needed.[3–5]

The objective of this study was to develop a highly sensitive analytical method that can quantify DBPs in wastewater-impacted waters at parts per trillion levels. To achieve this, we employed a gas chromatography tandem mass spectrometry technology that reduces background ions and targets specifically for selected ions resulting in lower detection limits. Tandem mass spectrometry is advantageous because it can produce "precursor ions" from a target analyte, select a precursor ion and further fragment it to "product ions". Quantification is based on selected product ions that have high signal to noise ratio that leads to a highly sensitive and selective method with almost no ambiguity. This highly sensitive quantification is advantageous for analysis of complex matrices such as secondary wastewater effluent where many contaminants and interferences exist in solution. Furthermore, we used this method to analyze DBP formation and DBP precursor removal throughout a full-scale wastewater reuse facility that uses microfiltration, ozonation, and reverse osmosis. This research is the first to comprehensively evaluate emerging DBP formation potential from chlorination and chloramination across a full-scale reuse facility.

2. Material and methods

2.1. Reagents and solutions

DBP analytical reference materials listed in Table 1 were obtained at the highest purity available from Sigma Aldrich (St. Louis, MO), Toronto Research Chemicals (Toronto, ON, Canada), AccuStandard (New Haven, CT, USA), and Cansyn Chem. Corp. (Toronto, ON, Canada). Anhydrous acetonitrile and methyl *tert*-butyl ether (MTBE) were purchased from Acros Organics (New Jersey, NJ, USA). Ultrapure water (≥18.1 MΩ) was obtained from a Barnstead MicroPure system (Thermo Fisher Scientific, USA).

Individual reference standards were weighted and diluted in anhydrous acetonitrile to make ~4000 mg L^{-1} stock solutions. Five 100 mg L^{-1} stock solutions for each DBP chemical class were prepared by mixing individual components in anhydrous acetonitrile. DBP chemical classes included haloacetonitriles (HANs), haloketones (HKTs), haloaldehydes (HALDs), halonitromethanes (HANs), and iodo-trihalomethanes (I-THMs). For example, a 100 mg L^{-1} stock mix of HALDs contained a mixture of dibromochloroacetaldehyde, bromodichloroacetaldehyde, and tribromoacetaldehyde. Individual and DBP mix stock solutions were stable for a year. Two master stocks were prepared daily prior to use by combining each DBP class to make 100 and 5 μg L^{-1} solutions. Master stocks were used to prepare neat standards in acetonitrile to spike ultra pure water samples.

2.2. Instrumentation

A gas chromatograph tandem mass spectrometer (GC-MS/MS) was used to quantify DBPs. The GC was an Agilent 7890B with multi-mode inlet (MMI) coupled to a 7000C Agilent triple quadrupole (Agilent Technologies, Santa Clara, CA). This system's ionization source was electron ionization (EI). The GC column used in this study was a Restek 200-Rtx column (30 m × 0.25 mm ID × 0.25 μm df) containing an inert mid-polarity crossbond trifluoropropylmethyl polysiloxane stationary phase. Previous studies[37,38] have shown the advantages of this mid-polarity column when analyzing several DBP chemical classes. The GC oven program started at 35 °C and was held for 5 min, followed by a temperature ramp of 9 °C min^{-1} to 220 °C. A second temperature ramp of 20 °C min^{-1} to 280 °C was programmed with a final hold of 20 min for a total run time of 47.6 minutes. Samples were injected as a pulsed-splitless injection with an inlet temperature program. The initial inlet temperature was 35 °C and increased to 170 °C at a rate of

Table 1 Optimized parameters for all DBPs used in this method, including chemical transitions, dwell times, collision energies and recoveries in ultra – pure (18 MΩ water)

DBP class	DBP	Purity (%)	Abb.	Retention time (min)	MDLs (ng L^{-1})	Percent recovery[e]	Precursor (m/z)	Quantification ion		Qualification ion		Dwell time (ms)
								m/z	CE (eV)	m/z	CE (eV)	
HAN	Chloroacetonitrile	99.5[b]	CAN	4.14	5.7	126.8	75	48	5	40.1	15	21.1
	Bromoacetonitrile	99.8[b]	BAN	6.69	3.6	120.8	120.9	40.1	10	41.1	10	18.3
	Iodoacetonitrile	98.1[b]	IAN	9.64	6.3	108.4	166.9	40.1	21	41.1	42	12.5
	Dichloroacetonitrile	99.4[d]	DCAN	3.86	3.2	91.4	73.9	47	21	40.1	32	22.2
	Dibromoacetonitrile	95.9[d]	DBAN	8.9	68.9	153.1	117.9	90.9	21	40.1	35	14.6
	Bromochloroacetonitrile	95.8[d]	BCAN	6.46	3.7	89.2	73.9	47	21	40.1	32	18.3
	Trichloroacetonitrile	98.0[d]	TCAN	2.95	3.2	34.1	107.8	72.9	29	47	60	21.7
HNM	Dichloronitromethane	96.2[a]	DCNM	4.85	4.1	109.2	82.9	48	52	47	55	27.8
	Dibromonitromethane	92.5[a]	DBNM	9.29	2.3	77.7	172.8	91.9	59	93.9	59	16.7
	Bromochloronitromethane	92.3[a]	BCNM	7.29	4.1	92.9	128.9	48	50	47	50	19.8
HAL	Bromodichloroacetaldehyde	94.2[a]	BDCAld	5.5	50.0	87.7	82.9	47	34	48	48	18.8
	Dibromochloroacetaldehyde	90.3[a]	DBCAld	7.91	11.9	106.6	128.9	48	48	47	50	18.8
	Tribromoacetaldehyde	97.3[b]	TBAld	9.94	13.0	111.7	172.8	91.9	59	93.9	58	20.8
HKT	1,1-Dichloropropanone	95.5[d]	11DCP	4.69	25.7	108.5	82.9	47	43	48	43	23.3
	1,3-Dichloropropanone	99.9[a]	13DCP	9.76	6.8	122.6	77	49	9	48	43	12.5
	1,1,1-Trichloropropanone	98.7[d]	111TCP	7.64	30.6	62.9	124.9	97	9	82.9	9	18.8
	1,1,3-Trichloropropanone	85.0[c]	113TCP	10.87	7.5	134.2	77	49	10	47	46	40.8
	1-Bromo-1,1-dichloropropanone	96.0[c]	1B11DCP	9.68	56.2	84.7	124.9	97	2	43.1	22	20.8
	1,1,3,3-Tetrachloropropanone	92.7[a]	1133TeCP	11.74	5.5	138.2	82.9	47	43	48	34	33.3
I-THMs	Dichloroiodomethane	99.9[a]	DCIM	4.12	5.7	88.3	209.9	82.9	1	84.9	12	22.2
	Bromochloroiodomethane	99.0[a]	BCIM	6.4	7.5	72.1	255.9	128.8	2	130.8	11	15.4
	Dibromoiodomethane	93.9[a]	DBIM	8.52	2.0	69.9	172.8	91.9	57	93.9	57	18.8
	Chlorodiiodomethane	99.9[a]	CDIM	9.02	3.6	53.2	174.9	48	53	47	60	20.8
	Bromodiiodomethane	92.5[a]	BDIM	10.8	5.6	52.0	218.8	91.9	60	140	60	45.8
	Iodoform	99.0[b]	TIM	12.74	3.1	49.2	266.8	140	60	127	60	50.0
I.S.	1,2-Dibromopropane	97.0[b]	I.S.	6.31	N/A	N/A	120.9	92.9	30	41.1	10	16.3

[a] CanSyn Chem Corp. [b] Sigma Aldrich. [c] Toronto Research Chemicals. [d] AccuStandard. [e] Percent recoveries are for optimized conditions detailed in Table 3. I.S.: internal standard; N/A: not applicable; MDLs: method detection limits; Abb.: abbreviation.

360 °C min^{-1}, followed by a second ramp of 720 °C min^{-1} to a final temperature of 250 °C. The injection pulse pressure of 20 psi was held for 0.75 min followed by an immediate purge to split vent of 30 mL min^{-1}. The transfer line and ion source temperatures were 250 °C and 200 °C, respectively.

The ionic transitions in the mass spectrometer were optimized by running a full scan of each DBP to observe the ion fragmentation pattern in each mass spectra. The base peak or the second most abundant peak for all analytes was selected for a product ion scan. Once the product ion with the highest signal was obtained, parameters including collision energies, dwell times and time segments were optimized. The mass spectrometer was programmed under multiple reaction monitoring (MRM) mode with optimized parameters. Pure standards and sample extracts were analyzed using the Agilent Mass Hunter (version 8.0) software for quantitation.

2.3. Calibration and method detection limits

Calibration curve and method detection limits (MDLs) were determined from solutions prepared with ultra pure water that were spiked with the master stocks that contained all DBPs. 1,2-Dibromopropane (internal standard) was added to the final extracts (8 μL of 30 mg L^{-1} 1,2-dibromopropane MTBE solution to 200 μL MTBE dried extract). Calibration curve solutions were prepared daily with concentrations of 0.001, 0.005, 0.01, 0.025, 0.05, 0.10, 0.25, 0.50, 1, 5, 10, and 25 μg L^{-1}. The calibration curves were separated in two parts in order to ensure linearity across all points. For low level quantification, a calibration curve using points between 0.001–0.50 μg L^{-1} was used. Other compounds were quantified with the upper half calibration points with a calibration curve ranging from 0.50–25 μg L^{-1}. Each calibration curve had a coefficient of determination (R^2) greater than 0.99 and had a linear range of three orders of magnitude.

MDLs were determined by the standard deviation of $n = 7$ replicates multiplied by the 99% confidence interval of a one-sided Student's t-test as detailed elsewhere.[38] Briefly, MDLs were calculated using the equation below. Where CL is the concentration of all replicates in μg L^{-1}, $t_{N-1,1-\alpha=0.99}$ is the 99% confidence level of $n - 1$ Student's t-value, and $SD_{PeakArea}$ and $AV_{PeakArea}$ are the averaged standard deviation and peak areas, respectively. MDLs are reported on Table 1.

$$\mathrm{MDL} = t_{N-1,1-\alpha=0.99}\mathrm{CL}\frac{\mathrm{SD}_{\mathrm{PeakArea}}}{\mathrm{AV}_{\mathrm{PeakArea}}}$$

2.4. Water samples & formation potential testing

Wastewater effluents were collected from Advancing Canadian Wastewater Assets (ACWA), a full-scale advanced

tertiary wastewater treatment that treats secondary wastewater effluents with microfiltration (UF) membranes (pore size 0.02 mm), followed by reverse osmosis (RO) or ozone treatment (O_3). The average ozone concentration was 1.20 mg L^{-1} at the time of sampling. The wastewater treatment process includes screen and grit removal, primary clarifier, activated sludge reactor, and secondary clarifier. Samples were collected in 1 L HDPE bottles with no headspace and were stored at 4 °C. Water quality parameters are shown in Table 2. Samples were extracted with optimized conditions and analyzed for DBPs as controls prior to formation potential testing.

Formation potential testing was performed under uniform formation conditions (UFC) to compare DBP formation across four different water matrices using chlorination (HOCl) and chloramination (NH_2Cl).[41] Briefly, water samples were filtrated through 0.45 μM polyethersulfone membrane disc filters prior to disinfection. All reagents were prepared using ultra pure chlorine demand free water (CDFW) to prevent any consumption of disinfectant by reagents. Hypochlorite dosing solutions (6500 mg L^{-1} as Cl_2) and chloramine (1000 mg L^{-1} as Cl_2) were prepared daily as explained elsewhere.[42,43] Filtered samples (400 mL) were spiked with 0.8 mL of 1 M borate buffer and adjusted to an overall pH of 8.0 ± 0.2 using H_2SO_4/NaOH solutions. Dosed samples were transferred to 125 mL amber bottles without headspace and incubated for 24 ± 1 h to achieve a chlorine residual between 0.60–1.40 mg L^{-1} as Cl_2 (Table 2). Chlorine residual and dosing solutions were quantified using a colorimetric standard method 4500-Cl.[44] All samples were quenched with 1.5 : 1.0 molar ratio of ascorbic acid to Cl_2 once the chlorine residual was measured (Table 2).[45] Quenched samples were immediately extracted and quantified in triplicate following the final extraction conditions detailed in Table 3.

2.5. Total organic halogen method

The total organic halogen method was followed as outlined in Kimura *et al.* with the following modifications.[46] The furnace program for the activated carbon (AC) columns was changed to 500 seconds at the end position, 200 seconds at the cooling position, and 200 seconds at the home position with argon and oxygen flow rate of 200 and 400 mL min^{-1}. A 0.02 mM ammonium buffer was used as the absorption solution to collect the furnace off-gases. The absorption solution was analyzed for chloride, bromide, and iodide using a Dionex Integrion Ion Chromatograph (Thermo Fisher Scientific, USA) and a 2 mm Dionex ADRS 600, anion dynamically regenerated suppressor was used. The chromatographic column used was a Dionex IonPac AS20 Analytical Microbore Column (250 mm × 2 mm ID).

3. Results and discussion

3.1. MS/MS optimization

3.1.1. Transitions. Individual DBP neat standards were first analyzed in full scan mode to identify DBP transitions and determine retention times. The precursor ions were selected based on the base peak (most abundant ion) for most DBPs. However, the precursor ion for 1,1-dichloropropanone (11DCP), 1,1,1-trichloropropanone (111TCP), 1-bromo-1,1-dichloropropanone (1B11DCP), dichloroiodomethane (DCIM), and bromochloroiodomethane (BCIM) were selected based on the second strongest fragment peak. For example, 11DCP, 111TCP, and 1B11DCP all shared a common *m*/*z* base peak of 43.1 representing the $[COCH_3]^+$ fragment. This fragment was not selected because upon further fragmentation, the *m*/*z* of the product ions would be less than 32. A similar issue was encountered for DCIM where the *m*/*z* base peak of $[Cl_2CH]^+$ 82.9 led to a weak product ion response. For this reason, the *m*/*z* molecular ion peak $[CHCl_2I]^+$ 209.9 was selected as the precursor ion. BCIM had a base peak of *m*/*z* 126.9 that corresponded to $[I]^+$ ion. The selection of the 126.9 *m*/*z* peak was not possible for further fragmentation, therefore the molecular ion $[CHBrClI]^+$ with *m*/*z* of 255.9 was selected as the precursor ion. After the precursor ion selection, a product scan was obtained to determine the fragmentation pattern and select the two most abundant *m*/*z* ions as the quantification (*Q*) and qualification (*q*) ion. Results are shown in Tables 1 and S1 in ESI.†

3.1.2. Collision energies. After DBP transitions were identified, collision energies (CE) were optimized to maximize the signal for each transition. First, HANs were

Table 2 Water quality parameters for each sample matrix analyzed, as well as the residual concentration of disinfect in each sample after 24 hours of disinfection incubated at 20 ± 1 °C. Initial and final disinfectant refers to the disinfectant concentration at t = 0 and after 24 hours, respectively. Disinfectant concentration was determined using the DPD colorimetric method

Matrix	DOC (mg L^{-1} as C)	TN (mg L^{-1} as N)	NH_3 (mg L^{-1})	pH	Chloride (mg L^{-1})	Bromide (μg L^{-1})	Initial/final disinfectant concentration (mg L^{-1} as Cl_2)	
							HOCl	NH_2Cl
Secondary wastewater effluents	7.38	8.53	0.91	7.2	121	55.6	10.33/1.02	2.21/1.20
Microfiltration	7.27	7.56	0.07	7.2	119	82.8	10.18/1.19	2.18/0.76
Microfiltration/ozonation	6.01	7.74	0.13	7.1	124	39.6	8.41/1.41	1.80/1.10
Microfiltration/reverse osmosis	<1.00	0.35	<0.04	5.7	3.48	1.54	1.00/0.81	1.00/0.79

DOC: dissolved organic carbon. TN: total nitrogen. Iodide was not detected in samples.

Table 3 Sample extraction: initial and final conditions

Variable	Initial conditions[a]	Final conditions[b]
Sample volume	100	10
Organic solvent	5 × 3	3 × 3
Sodium sulfate (g)	30	3
Shake time (min)	15	10
Rest time (min)	15	5
Total extraction time (6 samples in duplicate)	4 hours	2 hours

[a] (Cuthbertson *et al.*, 2020).[37] [b] This study.

optimized manually by incrementing the collision energy applied to each precursor ion. The CE was optimized once the maximum abundance was observed for the quantifier and qualifier transitions as shown in Fig. S1.† Manual optimization of CE values were compared to MassHunter's automatic "MRM transition optimizer" feature reported in Table 1. The automated CE values selected for the HANs class were in agreement with the manually optimized CE values, thereby validating the automated optimizer feature on Agilent's MassHunter. The MRM transition optimizer was then applied for the remaining DBPs. The optimizer feature varied the CE with increments of 2 eV with range between 0–60 eV. The software identified the CE that resulted in the highest abundance for each transition. All optimized CE are displayed in Table 1.

3.1.3. Time segments. In order to increase sensitivity of the instrument, time segments were introduced into the method. Time segments ensure higher sensitivity of the triple quadrupole by reducing the number of chemical transitions to scan for per segment.[47] A total of four time segments were included as shown in Fig. 1: 0.00–5.20, 5.20–8.20, 8.20–10.20, and 10.20–47.60 minutes. Each time segments had 6, 7, 8, and 4 DBPs, respectively. Additionally, each segment was selected when target peaks were not present (Fig. 1). The time gap between the peaks ensured that the quadrupoles and software had enough time to adjust for the scans included in the next segment.

3.1.4. Dwell times. Another parameter that was optimized for this method was the dwell time for each analyte. Dwell time refers to the sampling or scanning time spent for each peak during the MRM.[48] Typically, longer dwell times result in a higher number of ion hits to the detector resulting in an increased sensitivity of the analyte. Peak shape is dependent on dwell times as seen in the equation below

$$\text{Dwell time (ms)} = \frac{\text{pw}}{\text{tr} \times 15}$$

where, pw is the peak width in milliseconds, and tr is the number of total transitions in each time segment. Literature reports that 12–20 points per peak results in an acceptable peak shape that increases accurate quantitation and reproducibility of peak shape.[49,50] In our study, 15 data points were used in the equation to determine appropriate dwell time. For example, in the first time segment there were six analytes with two transitions each which corresponded to

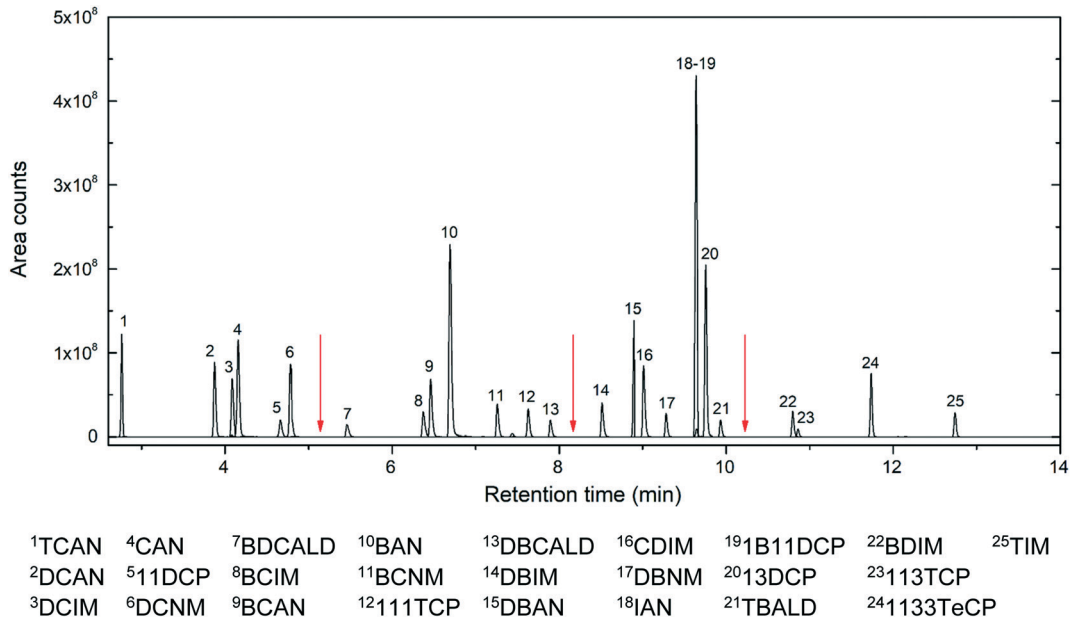

Fig. 1 Chromatographic separation of 25 DBPs from 1 mg L^{-1} in MTBE. Red arrows indicate time segments.

a total of 12 transitions per segment. The range of dwell times is due to the number of transitions per time segment resulting with dwell times between 12.5–50.0 ms as observed in Table 1. Chromatographic separation of all analytes with optimized collision energy, segment time and dwell time are shown in Fig. 1.

3.2. Sample extraction optimization

DBPs are small volatile molecules that are extracted with liquid–liquid extraction (LLE).[35–40] However, LLE is time consuming and is typically the limiting step for DBP analysis for most cases. Previously reported LLE method was further optimized in this study, to reduce time and resources increasing analysis capacity.[37] Due to the increased sensitivity that comes with a MS/MS system, the sample extract concentration was reduced, thereby requiring less sample and solvent volume, reagents, and overall analysis time. First, three sample volumes (100, 50 and 10 mL) were evaluated under similar conditions (Exp. 1, 2, and 4) as described in Table S2 in ESI.† Sodium sulfate was adjusted according to the sample volume to achieve salt saturation of 0.3 g mL^{-1}. LLE was performed in triplicate with 3 × 5 mL of MTBE (Exp. 1–3) and 3 × 3 mL MTBE (Exp. 4). Percent recoveries are reported in Table S3 in ESI† for all DBPs and plotted for I-THMs in Fig. 2a. In general, percent recoveries were reduced by about half when sample volume was reduced from 100 (Exp. 1) to 50 mL (Exp. 2). The reduction in recovery was likely due to a 50% more headspace volume using 125 mL amber bottles, where DBPs might have volatilized. However, when sample volume was reduced to 10 mL (Exp. 4, 40 mL amber vial was used) similar percent recoveries were obtained compared to 100 mL sample volume. Similar results were also observed with HNMs and HALDs therefore, a sample volume of 10 mL was used for further optimization. Additionally, two final extract volumes, 200 and 100 μL, were also evaluated (Exp. 2 and 3). Percent recoveries obtained in experiment 3 were slightly higher compared to experiment 2 however, a final volume of 100 μL was found difficult to work with during the nitrogen blowdown that could lead to a higher error in the method. Therefore, a final extract volume of 200 μL was used.

Solvent volume (1, 3, and 5 mL) and shaking time (5, 10, 15 min) were also optimized. LLE was performed three times for each solvent volume with MTBE. Percent recoveries are shown in Fig. 2b, S2, and S3 in ESI.† Initial extraction conditions of 5 mL × 3 for 15 min (Fig. S2†) had the best analyte percent recoveries (>70%) except for trichloroacetonitrile (TCAN). Similar results were observed with a lower solvent volume of 3 mL × 3 as shown in Fig. 2b. The majority of analytes had recoveries >70% for a 10 and 15 min shake times. Although reducing solvent volume may adversely affect analyte extraction efficiency from water samples, it can also reduce time required to concentrate the extract thereby minimizing analyte loss due to volatilization. However, when 1 mL × 3 was evaluated percent recoveries were significantly lower than 70% (Fig. S3 in ESI†). Therefore, solvent volume and shaking time was optimized at 3 mL × 3 and 10 minutes, respectively. Optimized sample extraction conditions are summarized in Table 3 which reduced overall sample extraction time by half compared to initial conditions (experiment 1).

3.3. Method validation and reproducibility

Analyte percent recoveries for 100 ng L^{-1} spikes for initial and optimized conditions (Table 3) are shown in Fig. 3a. Recoveries were calculated by comparing the area counts of a neat peak and an extracted peak. Extracted samples of ultra pure blanks did not contain target DBPs. Table S4† contains the standard deviation and relative standard deviation (RSD) in ultra pure water. Initial percent recoveries determined in

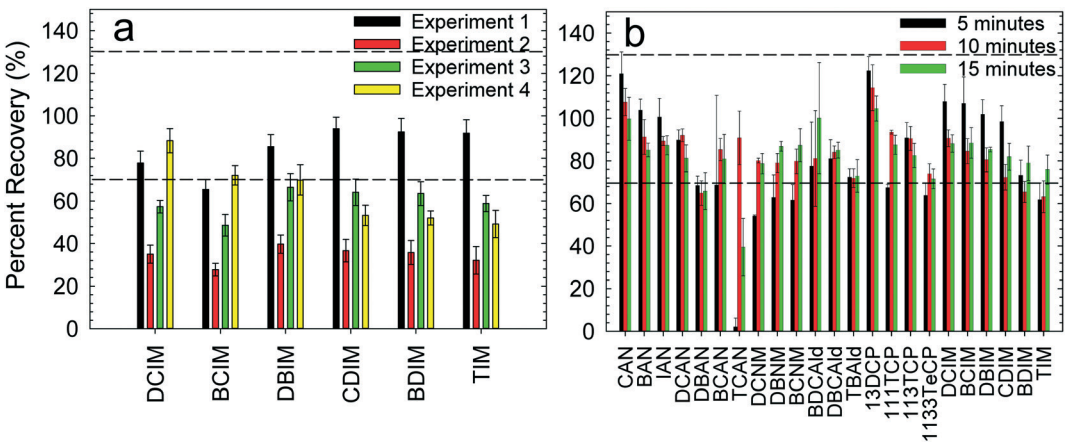

Fig. 2 a) Optimization of sample volume for I-THM class reported as percent recoveries. Dashed lines represent acceptable percent recovery range between 70–130%. Sample volumes were 100, 50, 50 and 10 mL for experiments 1–4, respectively. Organic solvent volumes were 15, 15, 15, and 9 mL for experiments 1–4. Final extract volumes were 200, 200, 100 and 200 μL for experiments 1–4, respectively. b) Optimization for three shake times for 3 mL × 3 of MTBE solvent extraction. All recoveries were performed in triplicate and average recovery is plotted. Dashed lines represent the acceptable range for DBPs (70–130%).

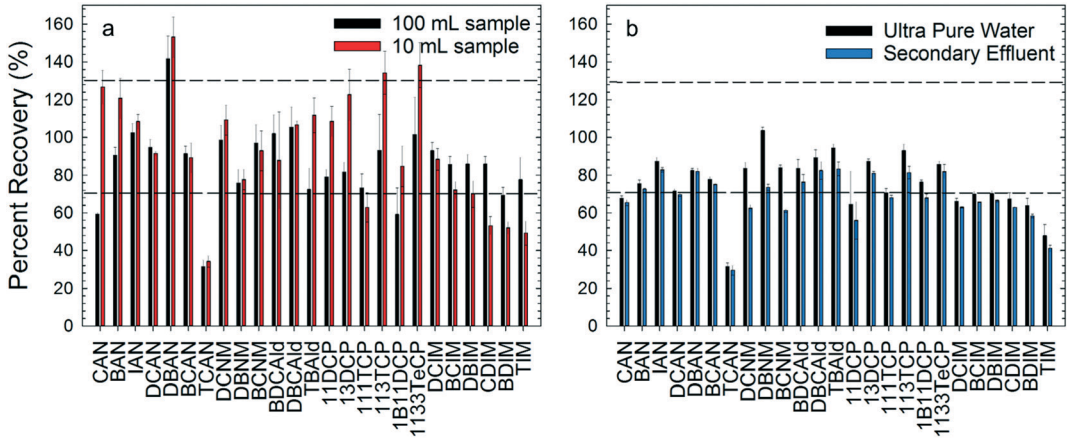

Fig. 3 a) Percent recoveries obtained from 100 ng L^{-1} spikes of analytical standards in ultra-pure water. Extractions were performed in triplicate and results are shown as an average. Dashed lines represent acceptable percent recovery range between 70–130%. b) Percent recoveries obtained from 5 μg L^{-1} spikes of analytical standards in ultra-pure water (black bars) and secondary effluent (blue bars). Extractions were performed in triplicate and results are shown as an average.

this study ranged between 31–142% which agrees with values obtained by Cuthbertson *et al.* between 30–110%.[37] TCAN had the lowest recovery at 31.3% which is slightly higher than previously reported at 20%. TCAN low recovery might be linked to TCAN's lower boiling point (84 °C) that indicates a higher volatility compared to other HANs that have boiling points ≥110 °C. In the sample extraction process, solvent extracts are blown down under a slow nitrogen stream where TCAN could have been lost in the process. Under optimized conditions, we observe that percent recoveries for 16 DBPs remain about the same especially for I-THMs. Higher recoveries were also observed for chloroacetonitrile (CAN), bromoacetonitrile (BAN), and 1,3-dichloropropanone (13DCP). However, dibromoacetonitrile (DBAN), dichloronitromethane (DCNM), bromochloronitromethane (BCNM), 1,1,3,3-tetrachloropropanone (1133TeCP), bromodichloroacetaldehyde (BDCALD), and dibromochloroacetaldehyde (DBCALD) had lower percent recoveries compared to initial conditions. The final optimized conditions obtained percent recoveries within 70–130% (ref. 37 and 51) except for DBAN, TCAN, 111TCP, 113TCP, 1133TeCP, iodoform (TIM), BDIM, DBIM and, CDIM. Furthermore, percent recoveries at a higher spike level of 5 μg L^{-1} at optimized conditions (Fig. 3b – ultra pure water) were between 31–104%. This method has the lowest reported MDLs between 2.0–68.9 ng L^{-1} (Table S9 in ESI†).

A study was performed to observe the reproducibility and precision of the analytical method. An acceptable precision is acceptable when the RSD is about 10% or less. Precision of the instrument was also tested for all analytes at a low (100 ppt) and mid, (250 ppt) and high concentrations (100 ppb). Replicate injections (n = 7) of all analytes were injected from the same vial to test the precision of the instrument. Precision was calculated by displaying the % RSD for each analyte at each concentration listed below in Table S5 in ESI.† The majority of analytes displayed low RSD (<3.1%) with higher concentrated samples however, TCAN displayed high RSD with an average of 60% for all spikes.

3.4. Matrix effects by secondary wastewater effluents

Sample extraction from different matrices other than ultra pure water could affect the efficiency to recover analytes. Fig. 3b illustrates the recovery of each analyte from ultra-pure water and secondary wastewater effluent. DBP percent recoveries from secondary effluents (29–83%) for most analytes were only slightly lower compared to ultrapure water extractions (31–104%). HNM percent recovery dropped from 84–104% in ultra pure water to 61–73% in wastewater effluents. However, calibration curves are obtained from known spiked ultra pure (18.2 MΩ) waters that undergo the sample extraction process. For this reason, although absolute percent recoveries determined in Fig. 3b are important, the main concern for the method's precision is the difference between both matrices. The difference between ultrapure and wastewater recoveries were between 0.5–30% which is acceptable. This might be explained due to the low sample volume (10 mL) used to extract DBPs where a low amount of "other" compounds were extracted from wastewater resulting in low matrix effects.

3.5. Advance treatment of secondary wastewater effluents: DBP formation potential with HOCl and NH_2Cl

3.5.1. DBPs in advance treatment of secondary wastewater effluents. Water samples were collected from secondary wastewater effluents treated with microfiltration membranes (UF) followed by ozone (UF/O_3), and reverse osmosis (UF/RO). DBPs including CAN, DCAN, DCIM, BCIM, and DCNM (Fig. 4 , Table S6 in ESI†) were quantified in all samples. DCAN and DCIM were quantified in secondary wastewater effluents at 14.8 and 13.3 ng L^{-1}, respectively and were subsequently reduced after UF treatment. In contrast, CAN and DCNM were not present in secondary effluents but were quantified

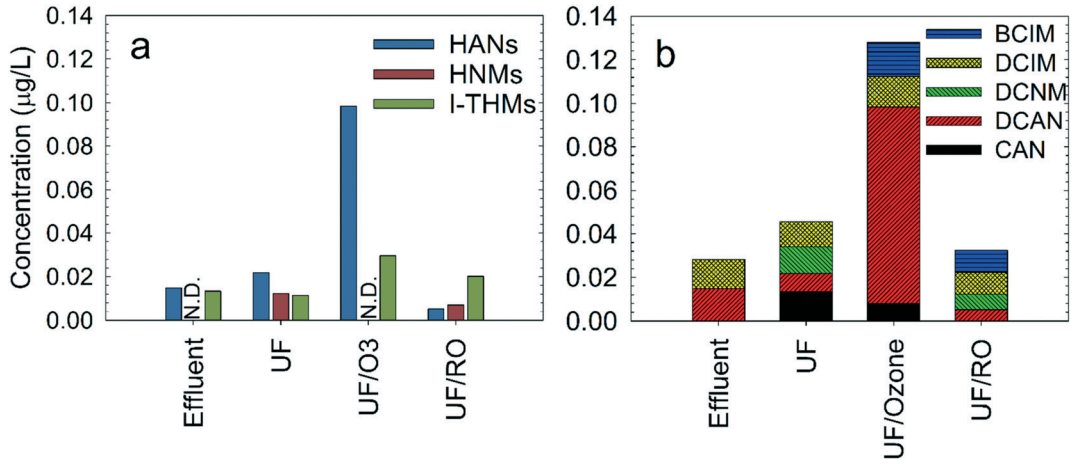

Fig. 4 Quantified DBPs in secondary wastewater effluents (effluent), microfiltration (UF), ozonation (UF/ozone), and reverse osmosis (UF/RO). DBPs are plotted a) by chemical classes, and b) individually stacked by sample.

after UF which suggests that CAN and DCNM were formed after UF. Previous studies have reported that during the backwashing/cleaning process of UF membranes with chlorine-based chemicals produced adsorbable organic halogen and trihalomethanes that leached into the permeate.[52,53] However, the detected DBPs were reduced overtime until non-detect concentrations (in the range of μg L^{-1}). It is possible that due to the higher sensitivity of the method used in this study (in the range of ng L^{-1}) was able to detect DBPs even after several days of operation after UF cleaning process.

UF/O_3 produced the highest DBP formation attributed primarily to HANs at 98.3 ng L^{-1} followed by I-THMs (29.6 ng L^{-1}). Although DCAN is reduced to 8.28 ng L^{-1} after UF treatment, it is re-formed after ozone treatment to a concentration of 90.3 ng L^{-1}. Non-halogenated and halogenated nitriles have been identified as a by-product in ozonation processes in drinking water.[2] However, this is the first time DCAN formation has been observed from ozonation in a reuse treatment facility. The enhanced HAN formation after ozonation was not observed in two other full-scale potable reuse facilities which might indicate that HAN formation could be unique to the composition of the effluent organic matter going through the facility in this study.[32]

After UF/RO treatment, DCAN, DCNM and DCIM levels were reduced between 14.7–43.4% compared to UF treatment alone. Additionally, BCIM was detected at 10.3 ng L^{-1} after UF/RO. A previous study that evaluated DBP rejection in RO membranes, found that DCAN, DCIM and BCIM exhibited the lowest DBP rejection at steady state ranging between ~40–50%.[54] DBPs detected in this study also agree with a poor RO rejection as reported by Doederer *et al.*[54]

Non-target analysis of the total organic halogen contained in water samples are shown in Fig. 5. The largest organic halide was TOCl with an average of 102.4 and 122.4 μg L^{-1} as Cl^- in secondary effluent and UF samples, respectively. Ozone and RO treatment removed 64.3 and 86.4% of TOCl compared to UF-treated samples. However, TOBr and TOI concentrations were consistent (6.6–7.0 μg L^{-1} as Br^- and 3.1–9.5 μg L^{-1} as I^-) in secondary effluent, UF, and UF/O_3 samples. UF/RO samples had no detectable TOBr and TOI but TOCl was still observed after UF/RO treatment. These results suggest the presence of halogenated organic contaminants such as pharmaceuticals and personal care products that are not well removed from wastewater secondary treatment and advanced treatment processes.[55,56]

3.5.2. DBPs formation potential with chlorine. Water samples were chlorinated according to UFC protocol to evaluate DBP formation potential and precursor removal of each treatment. A total of 12 of 25 DBPs were detected including HANs, I-THMs, HNMs, and HALDs as shown in Fig. 6 and Table S8 in ESI.† HKTs were not observed in any of the chlorinated samples. Secondary wastewater effluents and UF-treated waters had the highest DBP concentrations

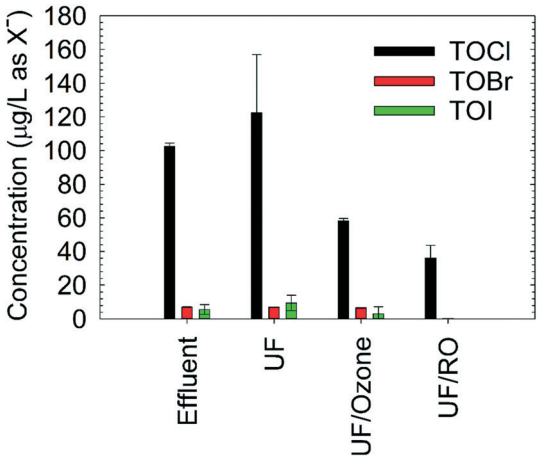

Fig. 5 Total organic halogen obtained from water samples without disinfection. TOCl, TOBr, and TOI are expressed in μg L^{-1} as Cl^-, Br^- and I^-, respectively. Analysis were performed in triplicate and results are shown as the mean and standard deviation.

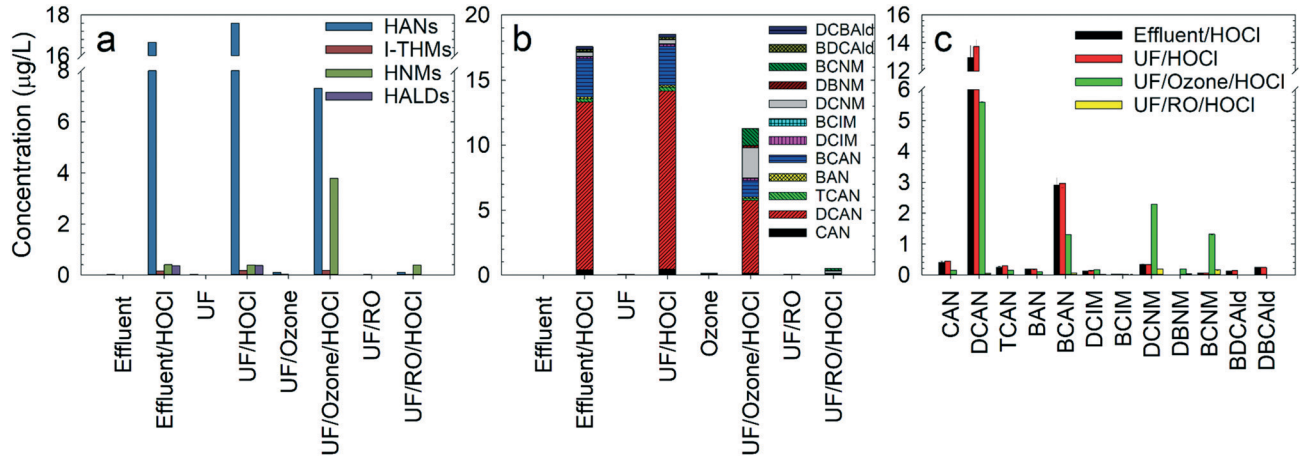

Fig. 6 Quantified DBPs after chlorination of secondary wastewater effluents (effluent/HOCl), microfiltration (UF/HOCl), ozonation (UF/ozone/HOCl), and reverse osmosis (UF/RO/HOCl). DBPs are plotted a) by chemical classes, b) individually stacked by sample, and c) individually.

(Fig. 6) in the order of HANs ≫ HNMs > HALDs > I-THMs. DBP speciation was found to be similar for both chlorinated samples which correlated with dissolved organic carbon and total nitrogen concentrations (Table 2). One possibility is that by filtering secondary wastewater effluents in the laboratory might have produced similar matrix/precursor composition to UF samples. Another possibility was that the UF membranes were not performing adequately at the time of sampling. However, ACWA quantified DOC on the same month as sampling and reported 8.46 and 6.76 mg L^{-1} as C for secondary wastewater effluent and UF treated samples, respectively. Therefore, sample prep filtration was the most likely explanation for similar DBP speciation for secondary wastewater effluent and UF samples. DCAN was the highest DBP with 12.9 and 13.7 μg L^{-1} in secondary wastewater effluents and UF treated waters, respectively. BCAN was the second highest DBP at a concentration of 2.92 and 2.96 μg L^{-1} for secondary wastewater effluents and UF, respectively. Additionally, total HNM, HAL and I-THMs levels were similar in secondary wastewater effluents and UF treated samples. Chlorinated effluent and UF samples formed 0.38–0.4 μg L^{-1} HNMs, 0.36–0.37 μg L^{-1} HALs, and 0.15–0.17 μg L^{-1} I-THMs.

UF/O_3/HOCl treated samples produced less DBPs compared to UF/HOCl (Fig. 6). However, total HAN (7.3 μg L^{-1}) was still the largest DBP chemical class with two major contributors, DCAN and BCAN that accounted for 77% (5.6 μg L^{-1}) and 18% (1.3 μg L^{-1}) of HAN formation, respectively. In comparison, ozonated water samples produced 42% less HANs than those quantified in UF-treated waters. These results suggest that ozonation is oxidizing amine precursors that lead to HAN formation. Similarly, other studies have also found that pre-ozonation followed by chlorination of effluent organic matter (EfOM) can decrease the formation of HANs with a simultaneous increase of HNM formation.[57–59] In our study, HNMs was the second largest DBP group with a total concentration of 3.8 μg L^{-1} were DCNM and BCNM accounted for 95% of the total. McCurry *et al.* proposed that ozonation can convert primary and secondary amines to nitroalkanes which can subsequently react with chlorine to form HNMs.[58] I-THMs were produced at significant lower levels than other DBP classes at 176.8 ng L^{-1} where DCIM accounted for ~90% of the total. I-THMs levels were similar to chlorinated secondary wastewater effluents and UF samples. Unexpectedly, HKTs and HALDs were not observed from UF/O_3/HOCl samples which might be related to the water's EfOM composition. A study conducted by Yang *et al.* found that pre-treatment with ozonation followed by chlorination of wastewater-impacted river waters enhanced the formation of haloketone 1,1,1-trichloropropanone (111TCP) and HALDs.[59]

UF/RO/HOCl samples exhibited significantly less DBP formation compared to the other treatments. This could in part be due to the lower DOC concentration in the sample (Table 2). RO was able to remove >85% of DOC which led to a lower DBP formation. Halonitromethanes were the most significant DBPs observed for chlorinated RO samples with DCNM and BCNM concentrations of 189 and 157 ng L^{-1}, respectively. HANs were also detected with concentrations of 52.5 and 53.1 ng L^{-1} for DCAN and BCAN, respectively. I-THMs were also observed with a total concentration of 26.3 ng L^{-1}.

3.5.3. DBP formation potential with chloramines. Chloramination of collected waters produced HANs, I-THMs, HNMs, and HKTs as shown in Fig. 7 and Table S7 in ESI.† HAN formation was significantly lower for chloraminated wastewater, UF, and UF/O_3 samples (0.33–0.55 μg L^{-1}) compared to chlorination (0.1–18 μg L^{-1}). Unlike chlorinated samples, chloramination enhanced HKT formation and HALDs however, HALDs were detected below their MDLs. Additionally, an increased I-THMs formation was observed after UF/O_3 and UF/RO compared to UF treated samples.

Secondary effluents and UF-treated waters exhibited similar DBP speciation trends and concentrations. 1,1-Dichloropropanone (11DCP) was the highest DBP formed

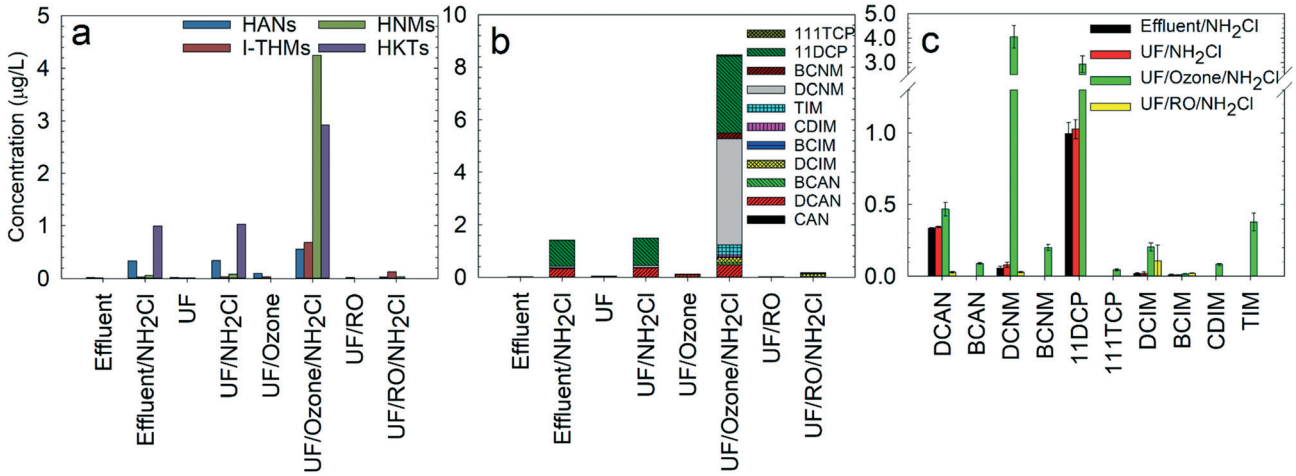

Fig. 7 Quantified DBPs after chloramination of secondary wastewater effluents (effluent/NH_2Cl), microfiltration (UF/NH_2Cl), ozonation (UF/ozone/NH_2Cl), and reverse osmosis (UF/RO/NH_2Cl). DBPs are plotted a) by chemical classes, b) individually stacked by sample, and c) individually.

in both waters with concentrations between 0.99–1.02 μg L^{-1}. DCAN was the second largest DBP for both waters ranging 0.33–0.34 μg L^{-1}. Similar trends were observed in Linge *et al.* study that detected 11DCP and DCAN in chloraminated secondary effluent and UF waters.[31] Other DBPs detected include DCIM, BCIM, and DCNM with concentrations between 0.009–0.08 μg L^{-1}.

UF/O_3-treated waters however, produced the highest DBP levels of all samples when disinfected with chloramines (Fig. 7). These results suggest that ozonation increases precursors that lead to a higher DBP formation. After a 24-hour chloramination, ozonated waters formed a total HNM concentration of 4.25 μg L^{-1} that included 4.05 μg L^{-1} DCNM and 0.20 μg L^{-1} BCNM. Song *et al.* also observed high HNM formation when secondary effluents underwent chloramination and ozonation–chloramination.[60] The pre-ozonation step resulted in a larger increase in HNMs consistent with this study. HKTs were the second largest forming DBP chemical class with a total concentration of 2.97 μg L^{-1} (Fig. 7a) composed by 11DCP and 1,1,1-trichloropropanone (111TCP). Total HAN (0.56 μg L^{-1}) increased after UF/O_3 compared to UF treated samples which included DCAN and BCAN. The increased formation of HANs in pre-ozonated waters is unusual as previous studies have shown that the pre-ozonation step reduced HAN precursors.[59,61,62] However, Yang *et al.* showed that waters with elevated bromide levels displayed an increase in HAN formation in pre-ozonated waters.[59] In this study, the UF/ozone water sample had 39.6 μg L^{-1} bromide which might had led to the formation of BCAN and therefore, an increase in HAN concentration. I-THMs in UF/O_3/NH_2Cl waters produced ~4× more I-THMs compared to UF/O_3/HOCl. It is well known that iodide in the presence of monochloramine can form HOI which can further react to produce I-THMs.[63,64] However, chlorine and ozone can readily oxidize hypoiodous acid (HOI) to iodate, a non-toxic iodine sink, that minimizes the formation of I-THMs. Furthermore, I-THMs were ~22× higher in UF/O_3/NH_2Cl waters than UF/NH_2Cl waters. These results indicate that iodine precursors might have been in the form or organic iodine (Fig. 5) instead of free iodide. Ozone can oxidize organic matter and increase I-THM precursors that subsequently react with chloramine to primarily form iodoform (TIM), followed by DCIM, CDIM, and BCIM. The tri-substituted TIM present in UF/O_3/NH_2Cl waters indicate that a relative high concentration of HOI oxidized organic matter multiple times leading to a high TIM concentration.

Similar to UF/RO/HOCl samples, UF/RO/NH_2Cl samples formed the least amount of DBPs compared to other treatments because of the efficient DOC removal by RO. Of all DBP classes formed, I-THMs was the largest DBP class attributed to DCIM with a concentration of 107 ng L^{-1} as seen in Fig. 6a and c. DCNM and DCAN were formed at similar levels at 29.9 and 27.3 ng L^{-1}, respectively and were the only HAN and HNM detected in these chloraminated waters.

4. Conclusions

A novel analytical GC-MS/MS method was developed that can analyze 25 DBPs at trace levels in treated wastewater effluents and recycled wastewater. This method has the lowest reported MDLs between 2.0–68.9 ng L^{-1} (Table S9 in ESI†) and is the first method to validate DBP analysis in wastewater effluents. There are very few studies that can comprehensively analyze multiple classes of DBPs because of the resource-intensive nature of analyzing several DBP classes with multiple analytical methods. Also, wastewater effluents are complex matrices that may introduce matrix effects that can be corrected through a laborious method known as standard addition.[65] For this reason, the method developed in this study is valuable because it can evaluate several DBP

chemical classes with low detection limits in complex water matrixes. However, the varying chemical properties of different classes of DBPs and their unstable nature (*i.e.*, volatile, light sensitive) resulted in a wide range of percent recoveries that were found to be similar to another multi-analyte DBP method for drinking water.[37] DBP percent recoveries were between 33.8–126.8% and 31–104% for water samples spiked with 100 ng L^{-1} and for 5 μg L^{-1}, respectively. The accuracy of this method could also be improved with isotopically labeled internal standards. However, these compounds are not commercially available and/or would need to be synthesized.

DBPs and DBP formation potential with chlorine and chloramines were evaluated for the first time throughout a full-scale wastewater reuse facility that included secondary wastewater effluent, UF, UF/O_3, and UF/RO waters. DCAN was quantified in secondary wastewater effluent which was removed by UF and reformed after UF/O_3. Chlorinated recycled waters produced high levels of HANs (~18 μg L^{-1}) which was ~20× higher than chloraminated recycled waters. Pre-ozonation enhanced HNM formation in UF/O_3/HOCl waters. HANs and HNMs were the most predominant DBPs quantified in UF/RO/HOCl treated waters. Chloraminated recycled waters predominantly formed HKTs however, when pre-ozonation was applied (UF/O_3/NH_2Cl), HNMs were the largest forming DBP class. UF/O_3/NH_2Cl produced the highest DBP levels compared to the other 3 treated waters. I-THM levels increased after UF/O_3/NH_2Cl and UF/RO/NH_2Cl treatment compared to UF/NH_2Cl treatment alone. The elevated DBP formation found in this study suggests that further investigation should be performed on recycled waters that includes the dependence on seasonability and wastewater effluent composition to evaluate the efficacy of DBP precursor removal.

Conflicts of interest

There are no conflicts to declare.

Acknowledgements

The authors are grateful for the funding provided by the University of Calgary, the Emerging Leader of America Program from Canada, and Natural Sciences and Engineering Research Council of Canada (NSERC) for this project. Continuous support from Restek and Dr. Tarun Anumol and Marcus Kim from Agilent Technologies also made this project possible. Water samples and water quality data were obtained from Advancing Canadian Wastewater Assets (ACWA), a full-scale advanced tertiary wastewater treatment facility, which was met with a tremendous amount of help from the operations and maintenance staff including Dr. Darina Kuzma, Dr. Andrea Scott, Dr. Leland Jackson, and Christine O'Grady. ACWA is a partnership between the University of Calgary and the City of Calgary – The City of Calgary is acknowledged for allowing construction of ACWA's facilities at a tertiary wastewater treatment facility. The authors would like to thank Dr. David Kinniburgh, Joanne Ye, and Xu Zhang from the Alberta Centre for Toxicology (ACFT) for their helpful suggestions throughout the development of this analytical method. Lastly, a warm thank you is extended to Dr. Jillian Murakami for her continuous help and discussions throughout the project, especially during the formation potential tests.

References

1 S. D. Richardson, M. J. Plewa, E. D. Wagner, R. Schoeny and D. M. DeMarini, Occurrence, genotoxicity, and carcinogenicity of regulated and emerging disinfection by-products in drinking water: a review and roadmap for research, *Mutat. Res.*, 2007, **636**, 178–242.

2 S. D. Richardson and T. A. Ternes, Water analysis: emerging contaminants and current issues, *Anal. Chem.*, 2011, **83**, 4614–4648.

3 S. D. Richardson and S. Y. Kimura, Water Analysis: Emerging Contaminants and Current Issues, *Anal. Chem.*, 2016, **88**, 546–582.

4 S. D. Richardson and T. A. Temes, Water Analysis: Emerging Contaminants and Current Issues, *Anal. Chem.*, 2018, **90**, 398–428.

5 S. D. Richardson and S. Y. Kimura, Water Analysis: Emerging Contaminants and Current Issues, *Anal. Chem.*, 2020, **92**, 473–505.

6 N. Costet, C. Villanueva, J. Jaakkola, M. Kogevinas, K. Cantor, W. King, C. Lynch, M. Nieuwenhuijsen and S. Cordier, Water disinfection by-products and bladder cancer: is there a European specificity? A pooled and meta-analysis of European case–control studies, *Occup. Environ. Med.*, 2011, **68**, 379–385.

7 R. Grazuleviciene, V. Kapustinskiene, J. Vencloviene, J. Buinauskiene and M. J. Nieuwenhuijsen, Risk of congenital anomalies in relation to the uptake of trihalomethane from drinking water during pregnancy, *Occup. Environ. Med.*, 2013, **70**, 274–282.

8 B. J. Horton, T. J. Luben, A. H. Herring, D. A. Savitz, P. C. Singer, H. S. Weinberg and K. E. Hartmann, The effect of water disinfection by-products on pregnancy outcomes in two southeastern US communities, *Occup. Environ. Med.*, 2011, **53**, 1172.

9 M. J. Nieuwenhuijsen, P. Dadvand, J. Grellier, D. Martinez and M. Vrijheid, Environmental risk factors of pregnancy outcomes: a summary of recent meta-analyses of epidemiological studies, *Environ. Health*, 2013, **12**, 6.

10 C. M. Villanueva, K. P. Cantor, S. Cordier, J. J. Jaakkola, W. D. King, C. F. Lynch, S. Porru and M. Kogevinas, Disinfection byproducts and bladder cancer: a pooled analysis, *Epidemiology*, 2004, 357–367.

11 C. M. Villanueva, K. P. Cantor, J. O. Grimalt, N. Malats, D. Silverman, A. Tardon, R. Garcia-Closas, C. Serra, A. Carrato and G. Castano-Vinyals, Bladder cancer and exposure to water disinfection by-products through ingestion, bathing, showering, and swimming in pools, *Am. J. Epidemiol.*, 2007, **165**, 148–156.

12 C. M. Villanueva, F. Fernandez, N. Malats, J. O. Grimalt and M. Kogevinas, Meta-analysis of studies on individual consumption of chlorinated drinking water and bladder cancer, *J. Epidemiol. Community Health*, 2003, **57**, 166–173.
13 K. Waller, S. H. Swan, G. DeLorenze and B. Hopkins, Trihalomethanes in drinking water and spontaneous abortion, *Epidemiology*, 1998, 134–140.
14 J. M. Wright, A. Evans, J. A. Kaufman, Z. Rivera-Núñez and M. G. Narotsky, Disinfection by-product exposures and the risk of specific cardiac birth defects, *Environ. Health Perspect.*, 2017, **125**, 269–277.
15 M. J. Nieuwenhuijsen, M. B. Toledano, N. E. Eaton, J. Fawell and P. Elliott, Chlorination disinfection byproducts in water and their association with adverse reproductive outcomes: a review, *Occup. Environ. Med.*, 2000, **57**, 73–85.
16 Health Canada, Guidelines for Canadian drinking water quality—Summary table, Water and Air Quality Bureau, Healthy Environments and Consumer Safety Branch, Health Canada, Ottawa, 2017.
17 S. D. Richardson and C. Postigo, in *Comprehensive Analytical Chemistry*, ed. S. Pérez, P. Eichhorn and D. Barceló, Elsevier, 2016, vol. 71, pp. 335–356.
18 N. J. P. Wawryk, C. B. Craven, L. K. J. Blackstock and X.-F. Li, New methods for identification of disinfection byproducts of toxicological relevance: Progress and future directions, *J. Environ. Sci.*, 2021, **99**, 151–159.
19 S. D. Richardson and M. J. Plewa, To regulate or not to regulate? What to do with more toxic disinfection by-products?, *J. Environ. Chem. Eng.*, 2020, 103939.
20 J. Rice and P. Westerhoff, Spatial and temporal variation in de facto wastewater reuse in drinking water systems across the USA, *Environ. Sci. Technol.*, 2015, **49**, 982–989.
21 J. Rice, A. Wutich and P. Westerhoff, Assessment of de facto wastewater reuse across the US: trends between 1980 and 2008, *Environ. Sci. Technol.*, 2013, **47**, 11099–11105.
22 X.-F. Li and W. A. Mitch, Drinking water disinfection byproducts (DBPs) and human health effects: multidisciplinary challenges and opportunities, *Environ. Sci. Technol.*, 2018, **52**(4), 1681–1689.
23 E. L. Marron, W. A. Mitch, U. V. Gunten and D. L. Sedlak, A tale of two treatments: the multiple barrier approach to removing chemical contaminants during potable water reuse, *Acc. Chem. Res.*, 2019, **52**, 615–622.
24 L. Alexandrou, B. J. Meehan and O. A. Jones, Regulated and emerging disinfection by-products in recycled waters, *Sci. Total Environ.*, 2018, **637**, 1607–1616.
25 Y.-H. Chuang and W. A. Mitch, Effect of ozonation and biological activated carbon treatment of wastewater effluents on formation of N-nitrosamines and halogenated disinfection byproducts, *Environ. Sci. Technol.*, 2017, **51**, 2329–2338.
26 Y.-H. Chuang, K. M. Parker and W. A. Mitch, Development of predictive models for the degradation of halogenated disinfection byproducts during the UV/H2O2 advanced oxidation process, *Environ. Sci. Technol.*, 2016, **50**, 11209–11217.
27 Y.-H. Chuang, A. Szczuka and W. A. Mitch, Comparison of toxicity-weighted disinfection byproduct concentrations in potable reuse waters and conventional drinking waters as a new approach to assessing the quality of advanced treatment train waters, *Environ. Sci. Technol.*, 2019, **53**, 3729–3738.
28 Y.-H. Chuang, A. Szczuka, F. Shabani, J. Munoz, R. Aflaki, S. D. Hammond and W. A. Mitch, Pilot-scale comparison of microfiltration/reverse osmosis and ozone/biological activated carbon with UV/hydrogen peroxide or UV/free chlorine AOP treatment for controlling disinfection byproducts during wastewater reuse, *Water Res.*, 2019, **152**, 215–225.
29 K. Doederer, W. Gernjak, H. S. Weinberg and M. J. Farré, Factors affecting the formation of disinfection by-products during chlorination and chloramination of secondary effluent for the production of high quality recycled water, *Water Res.*, 2014, **48**, 218–228.
30 S. W. Krasner, P. Westerhoff, B. Chen, B. E. Rittmann and G. Amy, Occurrence of disinfection byproducts in United States wastewater treatment plant effluents, *Environ. Sci. Technol.*, 2009, **43**, 8320–8325.
31 K. L. Linge, J. W. Blythe, F. Busetti, P. Blair, C. Rodriguez and A. Heitz, Formation of halogenated disinfection by-products during microfiltration and reverse osmosis treatment: implications for water recycling, *Sep. Purif. Technol.*, 2013, **104**, 221–228.
32 T. Zeng, M. J. Plewa and W. A. Mitch, N-Nitrosamines and halogenated disinfection byproducts in US Full Advanced Treatment trains for potable reuse, *Water Res.*, 2016, **101**, 176–186.
33 S. Dong, M. A. Page, N. Massalha, A. Hur, K. Hur, K. Bokenkamp, E. D. Wagner and M. J. Plewa, Toxicological comparison of water, wastewaters, and processed wastewaters, *Environ. Sci. Technol.*, 2019, **53**, 9139–9147.
34 Y. Du, W.-L. Wang, T. He, Y.-X. Sun, X.-T. Lv, Q.-Y. Wu and H.-Y. Hu, Chlorinated effluent organic matter causes higher toxicity than chlorinated natural organic matter by inducing more intracellular reactive oxygen species, *Sci. Total Environ.*, 2020, **701**, 134881.
35 C. M. Bougeard, E. H. Goslan, B. Jefferson and S. A. Parsons, Comparison of the disinfection by-product formation potential of treated waters exposed to chlorine and monochloramine, *Water Res.*, 2010, **44**, 729–740.
36 R. A. Carter, D. S. Liew, N. West, A. Heitz and C. A. Joll, Simultaneous analysis of haloacetonitriles, haloacetamides and halonitromethanes in chlorinated waters by gas chromatography-mass spectrometry, *Chemosphere*, 2019, **220**, 314–323.
37 A. A. Cuthbertson, H. K. Liberatore, S. Y. Kimura, J. M. Allen, A. V. Bensussan and S. D. Richardson, Trace analysis of 61 emerging Br-, Cl-, and I-DBPs: New methods to achieve part-per-trillion quantification in drinking water, *Anal. Chem.*, 2020, **92**, 3058–3068.
38 S. Y. Kimura, A. A. Cuthbertson, J. D. Byer and S. D. Richardson, The DBP exposome: Development of a new method to simultaneously quantify priority disinfection by-

products and comprehensively identify unknowns, *Water Res.*, 2019, **148**, 324–333.
39 S. W. Krasner, H. S. Weinberg, S. D. Richardson, S. J. Pastor, R. Chinn, M. J. Sclimenti, G. D. Onstad and A. D. Thruston, Occurrence of a new generation of disinfection byproducts, *Environ. Sci. Technol.*, 2006, **40**, 7175–7185.
40 H. S. Weinberg, S. W. Krasner, S. D. Richardson and A. Thruston Jr, The occurrence of disinfection by-products (DBPs) of health concern in drinking water: results of a nationwide DBP occurrence study, National Exposure Research Laboratory, Office of Research and Development, US Environmental Protection Agency, 2002.
41 R. S. Summers, S. M. Hooper, H. M. Shukairy, G. Solarik and D. Owen, Assessing DBP yield: uniform formation conditions, *J. - Am. Water Works Assoc.*, 1996, **88**, 80–93.
42 S. Y. Kimura, Y. Komaki, M. J. Plewa and B. J. Mariñas, Chloroacetonitrile and N,2-Dichloroacetamide Formation from the Reaction of Chloroacetaldehyde and Monochloramine in Water, *Environ. Sci. Technol.*, 2013, **47**, 12382–12390.
43 S. Y. Kimura, T. N. Vu, Y. Komaki, M. J. Plewa and B. J. Mariñas, Acetonitrile and N-Chloroacetamide Formation from the Reaction of Acetaldehyde and Monochloramine, *Environ. Sci. Technol.*, 2015, **49**, 9954–9963.
44 R. Baird, L. Bridgewater, A. American Public Health, A. American Water Works and F. Water Environment, *Standard methods for the examination of water and wastewater*, American Public Health Association, Washington, D.C., 23rd edn, 2017.
45 I. Kristiana, A. Lethorn, C. Joll and A. Heitz, To add or not to add: The use of quenching agents for the analysis of disinfection by-products in water samples, *Water Res.*, 2014, **59**, 90–98.
46 S. Y. Kimura, W. Zheng, T. N. Hipp, J. M. Allen and S. D. Richardson, Total organic halogen (TOX) in human urine: A halogen-specific method for human exposure studies, *J. Environ. Sci.*, 2017, **58**, 285–295.
47 P. Stone, T. Glauner, F. Kuhlmann, T. Schlabach and K. Miller, New Dynamic MRM Mode Improves Data Quality and Triple Quad Quantification in Complex Analyses, Agilent, 2009.
48 C. Nichols, B. Zekavat and P. Batoon, Instrument Detection Limit at Ultrashort Dwell Times Demonstrated on the Agilent 6495C Triple Quadrupole LC/MS, Agilent publication.
49 M. Kirchner, E. Matisová, S. Hrouzková and J. de Zeeuw, Possibilities and limitations of quadrupole mass spectrometric detector in fast gas chromatography, *J. Chromatogr. A*, 2005, **1090**, 126–132.
50 M. Sargent, Guide to achieving reliable quantitative LC-MS measurements, RSC Analytical Methods Committee, 2013.
51 M. M. Domino, B. V. Pepich, D. J. Munch, P. S. Fair and Y. Xie *Method 552.3. Determination of haloacetic acids and dalapon in drinking water by liquid-liquid microextraction, derivatization, and gas chromatography with electron capture detection*, Cincinnati, OH, 2003, USEPA 815-B-03-002, Revision 1.0.
52 P. Lipp, A. Schmitt and G. Baldauf, Treatment of soft reservoir water by limestone filtration in combination with ultrafiltration, *Desalination*, 1997, **113**, 285–292.
53 K. Hagen, Removal of particles, bacteria and parasites with ultrafiltration for drinking water treatment, *Desalination*, 1998, **119**, 85–91.
54 K. Doederer, M. J. Farré, M. Pidou, H. S. Weinberg and W. Gernjak, Rejection of disinfection by-products by RO and NF membranes: influence of solute properties and operational parameters, *J. Membr. Sci.*, 2014, **467**, 195–205.
55 M. Chen, V. Cooper, J. Deng, P. Amatya, D. Ambrus, S. Dong, N. Stalker, C. Nadeau-Bonilla and J. Patel, Occurrence of pharmaceuticals in Calgary's wastewater and related surface water, *Water Environ. Res.*, 2015, **87**, 414–424.
56 M. Chen, K. Ohman, C. Metcalfe, M. G. Ikonomou, P. L. Amatya and J. Wilson, Pharmaceuticals and endocrine disruptors in wastewater treatment effluents and in the water supply system of Calgary, Alberta, Canada, *Water Qual. Res. J. Can.*, 2006, **41**, 351–364.
57 A. Kozari, A. Paloglou and D. Voutsa, Formation potential of emerging disinfection by-products during ozonation and chlorination of sewage effluents, *Sci. Total Environ.*, 2020, **700**, 134449.
58 D. L. McCurry, A. N. Quay and W. A. Mitch, Ozone promotes chloropicrin formation by oxidizing amines to nitro compounds, *Environ. Sci. Technol.*, 2016, **50**, 1209–1217.
59 X. Yang, J. Peng, B. Chen, W. Guo, Y. Liang, W. Liu and L. Liu, Effects of ozone and ozone/peroxide pretreatments on disinfection byproduct formation during subsequent chlorination and chloramination, *J. Hazard. Mater.*, 2012, **239**, 348–354.
60 H. Song, J. W. Addison, J. Hu and T. Karanfil, Halonitromethanes formation in wastewater treatment plant effluents, *Chemosphere*, 2010, **79**, 174–179.
61 Y.-H. Chuang and H.-h. Tung, Formation of trichloronitromethane and dichloroacetonitrile in natural waters: precursor characterization, kinetics and interpretation, *J. Hazard. Mater.*, 2015, **283**, 218–226.
62 X. Yang, C. Shang, Q. Shen, B. Chen, P. Westerhoff, J. Peng and W. Guo, Nitrogen Origins and the Role of Ozonation in the Formation of Haloacetonitriles and Halonitromethanes in Chlorine Water Treatment, *Environ. Sci. Technol.*, 2012, **46**, 12832–12838.
63 Y. Bichsel and U. Von Gunten, Oxidation of iodide and hypoiodous acid in the disinfection of natural waters, *Environ. Sci. Technol.*, 1999, **33**, 4040–4045.
64 Y. Bichsel and U. Von Gunten, Formation of iodo-trihalomethanes during disinfection and oxidation of iodide-containing waters, *Environ. Sci. Technol.*, 2000, **34**, 2784–2791.
65 P. Makoś, A. Przyjazny and G. Boczkaj, Methods of assaying volatile oxygenated organic compounds in effluent samples by gas chromatography—A review, *J. Chromatogr. A*, 2019, **1592**, 143–160.